Diffusion of Single Star-Branched Dendrimer-like DNA

ARTICLE *in* THE JOURNAL OF PHYSICAL CHEMISTRY B · JUNE 2005

Impact Factor: 3.3 · DOI: 10.1021/jp0444924 · Source: PubMed

6 AUTHORS, INCLUDING:

Dan Luo
Cornell University
77 PUBLICATIONS **2,615** CITATIONS
SEE PROFILE

Pu Chun Ke
Monash University (Australia)
99 PUBLICATIONS **2,295** CITATIONS
SEE PROFILE

Article

Diffusion of Single Star-Branched Dendrimer-like DNA

Katherine O. Freedman, Janet Lee, Yougen Li, Dan Luo, Victoria B. Skobeleva, and Pu Chun Ke

J. Phys. Chem. B, **2005**, 109 (19), 9839-9842• DOI: 10.1021/jp0444924 • Publication Date (Web): 14 April 2005

Diffusion of Single Star-Branched Dendrimer-like DNA

Katherine O. Freedman,[†] Janet Lee,[†] Yougen Li,[‡] Dan Luo,[‡] Victoria B. Skobeleva,[§] and Pu Chun Ke*,[†]

Department of Physics and Astronomy, Clemson University, Clemson, South Carolina 29634, Department of Biological and Environmental Engineering, Cornell University, Ithaca, New York 14853, and Department of Polymer Sciences, Moscow State University, Leninskie Gory Moscow 119899, Russia

Received: December 3, 2004; In Final Form: February 1, 2005

We report a single-molecule fluorescence study on the diffusion of star-branched polymer dendrimer-like DNA (DL-DNA). The DL-DNA molecules were synthesized from ligating Y-shaped DNA to the fourth generation. It was found through single particle tracking that the diffusion coefficient of DL-DNA changes in a nonmonotonic fashion with its increased concentration possibly due to arm arrest and arm retraction. The diffusion of DL-DNA in linear lambda DNA solution displayed a monotonic concentration dependence 1 order of magnitude greater than the diffusion of DL-DNA in DL-DNA solution. This difference is attributed to the different conformation of DL-DNA and lambda DNA and the entanglement of lambda DNA with a large radius of gyration. Our diffusion study facilitates DL-DNA transportation for drug delivery.

Introduction

The diffusion of entangled polymer is often described by the reptation theory of de Gennes[1,2] and the tube model by Doi and Edwards.[3] In these models and their miscellaneous modifications, an entangled polymer crawls in a curvilinear and dynamic tube topologically confined by neighboring polymer chains. While these models were constructed mainly to describe the diffusion of flexible linear polymers, it is noted that many biopolymers and synthetic polymers are neither linear nor flexible (e.g., bacterial DNA, actin filaments, microtubules, and polyethylene). The complex nature of nonlinear polymers has often hindered our understanding of their diffusion and reptation.

The diffusion of nonlinear polymers such as star-branched or cyclic polymers has recently been explored. In particular, the theoretical treatments in connection with reptation theory have addressed the unique properties of star polymer solutions and melts on aspects such as arm retraction,[4,5] diffusion and relaxation,[6] scaling,[7] and structural arrest.[8] The experimental indications as to the molecular mechanism by which entangled stars relax have so far come mostly from viscoelastic data,[9] forward recoil spectrometry,[10] and neutron spin−echo spectroscopy.[11] For such molecules, reptation is expected to be severely suppressed and tube renewal may come to dominate the longest relaxation processes.[12] For this reason, studies of the diffusion or relaxation of nonlinear molecules in an entangled linear matrix may give more direct information on tube renewal processes than a corresponding study in a fully linear system. Furthermore, understanding the diffusion of nonlinear polymers may provide information to derive the scaling properties of polymer networks and other soft condensed matter systems, as well as facilitate the advent of rheology, drug delivery, and gel electrophoresis. For the very same argument, two systems, that is, nonlinear polymers diffusing in linear polymers and nonlinear polymers diffusing in nonlinear polymers, were experimentally examined in our study.

Dendrimers are star-branched, nonlinear macromolecules, which can be synthesized in a step-by-step fashion from a central core using repetitive chemistry. As with carbon nanotubes, dendrimers are yet another promising material from the realm of nanotechnology and can be used in a variety of applications. The most investigated dendrimers, mainly for the purpose of drug delivery, are the polyamidoamine (PAMAM) family.[13] The divergent synthesis of PAMAM dendrimers starts with an amine functional core unit that is reacted with methyl acrylate by Michael addition reaction.[13] Recently, a novel form of dendrimer, dendrimer-like DNA (DL-DNA), has been constructed through the ligation of Y-shaped DNA (Y-DNA).[14] These multivalent dendrimers represent a full achievement of DNA-based materials and can be synthesized either isotropically or anisotropically, providing great potential to link other entities such as prodrug and drug molecules. When triggered by a specific signal (chemical or radiation), a DL-DNA scaffold may fall apart in a chain reaction, yielding simultaneously biologically active end groups to the target. The base pairing capacity of DNA also holds promises for DL-DNA in molecular sensing and recognition.

Recently, the diffusion of a single flexible polymer, that is, DNA, in a matrix of flexible polymers,[15−17] and the diffusion of a single semi-flexible polymer, that is, an actin filament, in a solution of actin filaments[18] have been studied using laser tweezers and fluorescence microscopy. These single-molecule studies, complementary to ensemble approaches such as dynamic light scattering, NMR, and mass spectroscopy,[19−21] have enabled a direct visualization of the tube within which a polymer molecule reptates, and have provided a direct verification of the scaling laws of polymer diffusion and reptation with respect to polymer length and concentration.

In this Article, we report, to our knowledge, a first single-molecule study on the diffusion of star-branched polymers, DL-DNA, using EPI fluorescence microscopy. Our primary goal is to investigate, from the polymer physics viewpoint, the diffusion

* Corresponding author. E-mail: pcke11@clemson.edu.
[†] Clemson University.
[‡] Cornell University.
[§] Moscow State University.

10.1021/jp0444924 CCC: $30.25
Published on Web 04/14/2005

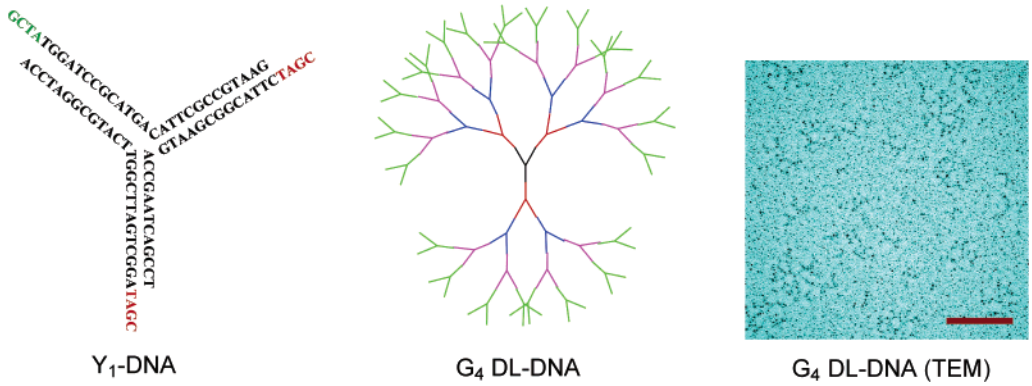

Figure 1. (Left) Structure of a Y_1-DNA molecule after hybridization of three oligonucleotides. The sticky ends of the oligonucleotides are shown in color. (Center) Structure of a G_4 DL-DNA molecule. (Right) TEM image of G_4 DL-DNA molecules (100 kV, stained with uranyl acetate and coated with approximately 10 nm Pt/Pd). Scale bar: 100 nm.

behavior of nonlinear star-branched polymer DL-DNA in response to the concentration of DL-DNA and linear polymer lambda DNA. Our study is to provide new data at the single-molecule level for the theoretical treatment of nonlinear polymers. Through this study, we also aim to provide physical guidance for the applications of nonlinear polymer DL-DNA in drug delivery.

Experimental Section

Synthesis of Fourth Generation Dendrimer-like DNA. The sequences of three oligonucleotides were designed such that half of each oligonucleotide was complementary to half of the others. After hybridization, these three oligonucleotides formed a three-arm junction or Y-DNA (Figure 1, left).[14] In addition, each Y-DNA consists of three nonpalindromic sticky ends so that it can only be ligated to other Y-DNA through Watson−Crick pairing. This nonpalindromic design prevents Y-DNA from self-ligation and ensures dendrimer synthesis is uni-directional. Thus, these Y-DNA molecules can be utilized as basic building blocks to synthesize DL-DNA with precise control. More specifically, the three sticky ends of core Y-DNA, Y_0-DNA, were complementary to only one sticky end of Y_1-DNA. After T4 DNA ligase (Promega) was added to the Y_0-DNA and Y_1-DNA mixture, three Y_1-DNA molecules were ligated to one Y_0-DNA, forming the first generation (G_1) DL-DNA. The two sticky ends of Y_1-DNA were left to be occupied by their complementary sticky ends of the next generation building blocks Y_2-DNA. Consequently, six Y_2-DNA molecules were ligated to one G_1 DL-DNA to form the second generation (G_2) DL-DNA. Likewise, the third generation (G_3) and the fourth generation (G_4) DL-DNA were synthesized (Figure 1, center).[21]

Y-DNA and different generations of DL-DNA formations were confirmed by the electrophoretic mobility retardation assays on agarose gels. The dendritic architecture of highly branched DL-DNA nanostructures was further characterized by transmission electron microscopy (TEM, Philips EM-201, see Figure 1, right) and atomic force microscopy (data not shown). The measured diameter of G_4 DL-DNA (83.9 ± 9.8 nm) from TEM was slightly larger than the theoretical calculated value (71.4 nm) due to metal coating.

Labeling of G_4 DL-DNA with POPO-3. The G_4 DL-DNA was labeled through intercalating with dye POPO-3 (1 mM in *N*,*N*-dimethylformamide, Molecular Probes, absorption 534 nm and emission 570 nm) in darkness at room temperature for 1 h. The dye−base molar ratio for the labeling is 1:5 in T4 DNA ligase buffer (30 mM Tris-HCl, pH 7.8, 10 mM $MgCl_2$, 10 mM DTT, and 1 mM ATP, Promega). Each G_4 DL-DNA is 2070 base pairs (bp) on average and is therefore estimated to be labeled with 414 dye molecules for sustained fluorescence emission. It is known that POPO-3 has a high binding affinity for nucleic acids and, upon excitation, emits fluorescence with a high quantum yield. Because POPO-3 is essentially nonfluorescent in the absence of nucleic acids, the possibility of imaging free dye molecules in the experiment was excluded. The labeling assay of DL-DNA with POPO-3 was confirmed with fluorescence microscopy.

Fluorescence Imaging. The labeled DL-DNA molecules were mixed uniformly with nonlabeled DL-DNA and nonlabeled lambda DNA (48.5 kbp or approximately 16 μm, 10 mM Tris-HCl, 0.1 mM EDTA, 5 mM NaCl, pH 7.4, Invitrogen), respectively. The T4 DNA ligase buffer, which has a viscosity close to that of water, was used for all dilutions. The concentrations of the polymer solutions, that is, the DL-DNA (labeled and nonlabeled DL-DNA) and the lambda DNA, were varied from 0.025 to 1.9 μg/μL and 0.1 to 1 μg/μL, respectively. A sample volume typically of 10 μL, composed of 0.2 μL of labeled DL-DNA solution of 0.0447 μg/μL and 9.3 μL of nonlabeled DL-DNA or lambda DNA solution of various concentrations, was flowed into a 5 mm wide channel made of double-sided tape (~150 μm thickness) sandwiched between a cover glass and a microscope slide. To reduce photobleaching of the labeled DL-DNA, approximately 0.5 μL of oxygen scavenger, propyl gallate (4% in water), was mixed uniformly to the sample cell, which was then sealed with nail polish and incubated in darkness for 30 min. After incubation, the sample slide was mounted on an EPI fluorescence microscope and the labeled DL-DNA was excited with green light (excitation filter 525AF45, Omega) from a mercury lamp (PTI, 100 W). The fluorescence emitted from the labeled DL-DNA was collected by a water immersion objective (Olympus, 60×, $NA = 1.2$) and focused onto a sensitive CCD camera (Roper, Cascade 512B). The field of view of the CCD camera was calibrated at 180×180 μm approximately. Typically 1−5 labeled DL-DNA molecules were observed per screen. The frame rate of the camera was set at 6 frames/s.

For single-molecule diffusion studies, a fluorescently labeled molecule can be followed at nanometer resolution via single-particle tracking (SPT).[22−26] In this scheme, the center of mass (COM) of a diffusing molecule, or a fluorescent spot on a detector (Figure 2a), is first determined by digitizing the image followed by Gaussian intensity profiling.[22] The two-dimensional (2D) mean-square-displacement (*MSD*) of the molecule is then obtained as $MSD(\Delta t) = \langle (x_{i+n} - x_i)^2 + (y_{i+n} - y_i)^2 \rangle$, where x_i and y_i are the position coordinates of the COM (Figure 2b) of

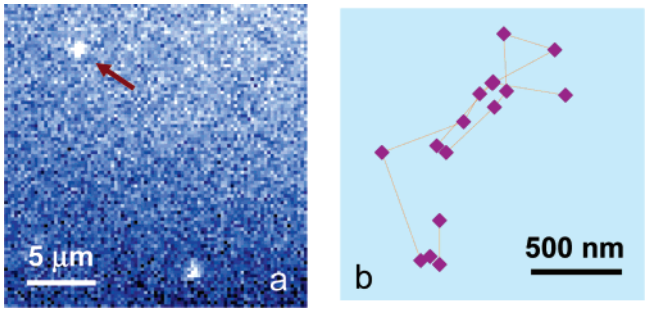

Figure 2. (a) A fluorescence image of two diffusing DL-DNA molecules. (b) Corresponding 2D trajectory of the indicated diffusing DL-DNA molecule in (a) over a time interval of 2.8 s.

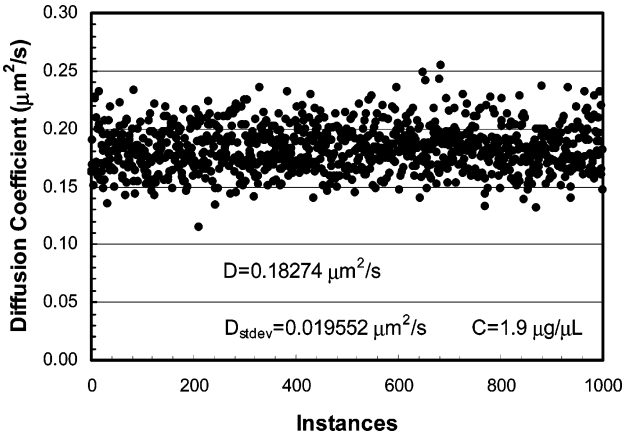

Figure 3. Bootstrap data analysis for labeled DL-DNA in DL-DNA solution of 1.9 μg/μL. The diffusion coefficient D is calculated for 1000 instances as 0.18274 μm^2/s with a standard deviation D_{stdev} of 0.019552 μm^2/s.

the molecule in frame i ($i = 1, 2, 3...$), and n denotes the frame number with time lapse Δt from frame i.[16,22] The diffusion coefficient D of the molecule undergoing 2D random walk[3] is finally derived as $D = MSD(\Delta t)/4\Delta t$ from linear curve fitting.[16,22] In our experiment, each fluorescent molecule was followed for 5 s (30 frames) for the low concentrations of DL-DNA to 10 s (60 frames) for the high concentrations of DL-DNA until the molecule drifted out of focus. The labeled molecules typically diffused within an area of 10×10 μm for the observed times. The system resolution/stability was calibrated to be 5×10^{-5} μm^2/s by imaging fluorescence beads immobilized on a glass substrate. The diffusion coefficient and its standard deviation of each data point were calculated on the basis of the bootstrap method[27] for 1000 times of iterations for a collection of approximately 100 molecules.[16] An example of data analysis using this method is given in Figure 3 for labeled DL-DNA in DL-DNA solution of 1.9 μg/μL. As shown in Figure 4, the diffusion coefficient D of DL-DNA solution was reduced from 0.64 to 0.18 μm^2/s when the concentration C of the DL-DNA solution was increased from 0.025 to 1.9 μg/μL. By comparison, the diffusion coefficient D of DL-DNA solution was reduced from 0.50 to 0.02 μm^2/s when the concentration C of the lambda DL-DNA solution was increased from 0.1 to 1 μg/μL. The diffusion of the DL-DNA solution showed a nonmonotonic behavior with the increased concentration of DL-DNA. In particular, an experimentally repeatable drop of diffusion coefficient D occurred near $C = 0.2$ μg/μL of DL-DNA solution, followed by relatively stable diffusion between $C = 0.2$ and 0.8 μg/μL of DL-DNA solution, and gradually reduced diffusion when $C > 0.8$ μg/μL for DL-DNA solution. By contrast, a monotonic reduction of diffusion coefficient was

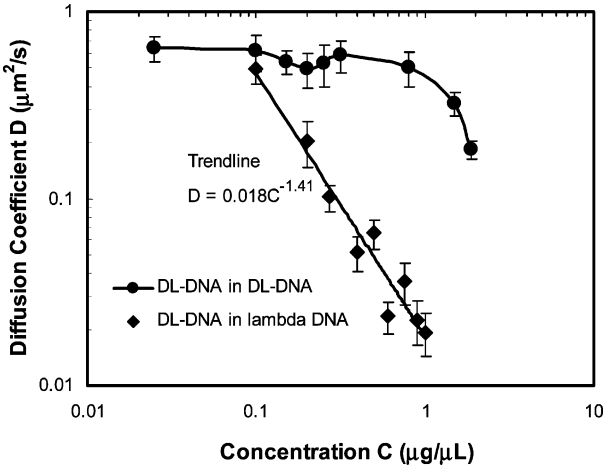

Figure 4. Diffusion coefficient of G_4 DL-DNA as a function of the concentration of G_4 DL-DNA (●) and lambda DNA (◆), respectively. Also shown in the plot are the trendline for the diffusion of DL-DNA in lambda DNA and the moving average for the diffusion of DL-DNA in DL-DNA. Each data point was measured with approximately 100 labeled G_4 DL-DNA molecules. The plot is in a log−log scale.

observed for labeled DL-DNA solution with increased concentration of lambda DNA. The power exponent of the trendline for DL-DNA solution is −1.41, when diffusing in lambda DNA solution of concentration between 0.1 and 1 μg/μL. It is known that the diffusion of lambda DNA starts to become constrained at a concentration of 0.4 μg/μL.[16] Above 1 μg/μL, the lambda DNA solutions were too viscous to pipet accurately and appear inhomogeneous. These factors might have contributed to the larger scattering of the data points when the concentration of lambda DNA is higher than 0.4 μg/μL (Figure 4).

Discussion and Conclusion

The conformation of flexible star polymers is known to be significantly different from that of homologous linear chains because topology has a great influence in local density. Hence, star polymers can be viewed as hybrids between soft flexible polymer-like entities and hard colloidal particles of two different domains of physics.[6,8] DL-DNA may be treated as a three-arm star polymer branched by its composing Y_1-DNA to Y_4-DNA submolecules. The mixture of labeled DL-DNA in nonlabeled, otherwise identical DL-DNA solution provides a model system for studying the diffusion of star-branched polymer, while labeled DL-DNA in lambda DNA solution represents a nonuniform ensemble of nonlinear polymers diffusing in linear polymers.

The differences in the linear and star chain mobility behavior at high concentration, as observed in Figure 4, are not only due to the size effect. It is noted in the dynamic Monte Carlo simulation with the bond fluctuation model by Cecca et al.[6] that the diffusion of star chains as a function of increased volume fraction Φ, a parameter related to star concentration, varies in an "irregular" fashion for $\Phi > 0.015$. As the star chains start to overlap, the slope of their diffusion coefficient displayed a plateau region followed by a more pronounced negative fall. By contrast, their parallel simulation on linear polymer chains showed only a linear reduction of the diffusion coefficient with the increase of polymer concentration.[6] In the molecular dynamics and Brownian dynamics simulations by Foffi et al.,[8] the self-diffusion coefficient of dense star-polymer solutions changes with their increased packing fraction or number density, in a nonmonotonic trend which resembles strikingly what we observed for the diffusion of DL-DNA in DL-DNA of increased

concentration, that is, an initial drop, followed by a slight rebound, then a plateau, and finally a gradual fall.

The complex diffusion behavior of DL-DNA in DL-DNA solution may be interpreted as a combined result of the star-branched conformation and the net negative charge of DL-DNA molecules. When the concentration of DL-DNA solution is increased ($C = 0-0.2$ μg/μL), DL-DNA molecules are brought within close proximity causing their negative charges to start to repel each other which may halt the diffusion, that is, a drop in diffusion coefficient. When the concentration of DL-DNA solution continues to rise so that their thermal agitation can overcome the initial repulsive potential, the stars and branches of the DL-DNA molecules may be rearranged in such a way that intermolecular diffusion is feasible, that is, a rebound in diffusion coefficient ($C = 0.2-0.314$ μg/μL). Further increase of the DL-DNA concentration relinquishes the space allocated for the arms and branches and causes the three arms and branches of the DL-DNA to retract possibly one at a time from entanglement. The former effect contributes to the suppressed diffusion, while the latter promotes diffusion/reptation. The overall effect is the nearly stalled diffusion coefficient (plateau, $C = 0.314-0.8$ μg/μL). Beyond this range when the concentration of DL-DNA solution becomes even higher, the stars and branches become so entangled/arrested with each other that their diffusion starts to reduce more significantly (the gradual drop, $C > 0.8$ μg/μL). Further increase of the concentration of DL-DNA, as suggested by the steep slope of diffusion coefficient versus concentration in Figure 4, would ultimately confine DL-DNA molecules to small spherical blobs and/or arrested clusters whose diffusion may resemble that of condensed small particles. Indeed, based on the molecular weight of the DL-DNA (2070 bp/molecule) and the sample volume ($\sim$10 μL) used in the experiment, and assuming the DL-DNA is elongated by $\sim$30% due to fluorescence labeling,[16] it can be estimated that at $C \approx 1$ μg/μL, the DL-DNA molecules within the sample cell become fully compacted.

The radius of gyration, R_G, of lambda DNA of approximately 700 nm is inferred from the diffusivity of stained DNA in dilute solution.[16] An entanglement of lambda DNA molecules is expected to occur at $C > 0.6$ μg/μL.[16] Using ξ to represent blob size, and n_e the number of blobs in an entanglement, the tube diameter a of entangled lambda DNA can be expressed as $a = \xi n_e^{1/2}$. Using the ratio of the entanglement concentration, c_e, to the overlap concentration, c^*, observed for lambda DNA molecules, and the scaling law as $c_e/c^* = n_e^{3\upsilon-1}$,[28,29] we can calculate n_e as $\sim$14 for lambda DNA. Here, υ represents the excluded volume exponent, which has the value of 0.588. At the overlap concentration, c^*, polymer coils begin to interact and the blob size, ξ, equals the size of the coil R_G. The tube diameter, a, can therefore be estimated as approximately 2.59 μm, which is significantly larger than the diameter of the DL-DNA molecule of 83.9 nm. Hence, for lambda DNA of concentration $C > 0.6$ μg/μL, the motion of DL-DNA can be viewed as hindered diffusion in a fixed matrix of entangled lambda DNA. The reptation of DL-DNA in linear lambda DNA solution is expected to be insignificant, as also indicated by the power exponent of -1.41 shown in Figure 4. Note the power exponent was predicted to be -1.75 by the reptation theory for entangled linear polymers. Hence, our result showed the departure from the reptation theory for star-branched DL-DNA diffusing in linear lambda DNA solution.

In summary, we have measured with fluorescence microscopy the diffusion of star-branched polymer DL-DNA, in nonlinear DL-DNA solution and linear lambda DNA solution. Our single-molecule study has unraveled the nonmonotonic concentration dependence for the diffusion of DL-DNA in DL-DNA solution, in close agreement with the theoretical simulations in the literature.[6,8] This irregular concentration dependence is explained as the combined result of the net negative charge and the conformation and interaction of DL-DNA including arm retraction and arm arrest. The diffusion of DL-DNA in linear lambda DNA solution, a system mimicking drug delivery with DL-DNA in cell nucleus, is regarded as hindered diffusion in a fixed matrix and found to deviate from the reptation theory constructed for linear polymers. Our single-molecule study sheds light on a better understanding of the diffusion of nonlinear polymers and facilitates drug delivery with nonlinear polymeric transporters.

Acknowledgment. P.C.K. acknowledges the support of a Russian Area Studies Grant and the startup funds from Clemson University. D.L. acknowledges the support of the Cornell University's Innovation Grant administrated by the Cornell Advanced Center for Biotechnology. We thank Christoph Naumann for insightful discussions and Qi Lu for critical reading of the manuscript.

References and Notes

(1) de Gennes, P. G. *J. Chem. Phys.* 1971, *55*, 572; *Macromolecules* **1976**, *9*, 587; *Phys. Today* **1983**, *36*, 33.
(2) de Gennes, P. G. *Scaling Concepts in Polymer Physics*; Cornell University Press: Ithaca, New York, 1979.
(3) Doi, M.; Edwards, S. *The Theory of Polymer Dynamics*; Clarendon: Oxford, 1986.
(4) Brochard-Wyart, F.; Ajdari, A.; Leibler, L.; Rubinstein, M.; Viovy, J. L. *Macromolecules* **1994**, *27*, 803.
(5) Milner, S. T.; McLeish, T. C. B. *Macromolecules* **1997**, *30*, 2159.
(6) Cecca, A. D.; Freire, J. J. *Polymer* **2003**, *44*, 2589.
(7) Schulte-Frohlinde, V.; Holovatch, Y.; von Ferber, C.; Blumen, A. *Phys. Lett. A* **2004**, *328*, 335.
(8) Foffi, G.; Sciortino, F.; Tartaglia, P.; Zaccarelli, E.; Lo Verso, F.; Reatto, L.; Dawson, K. A.; Likos, C. N. *Phys. Rev. Lett.* **2003**, *90*, 238301-1.
(9) Ferry, J. D. *Viscoelastic properties of polymers*, 3rd ed.; Wiley: New York, 1980.
(10) Shull, F. R.; Kramer, E. J.; Fetters, L. J. *Nature* **1990**, *345*, 790.
(11) Stellbrink, J.; Allgaier, J.; Monkenbusch, M.; Richter, D.; Ehlers, G.; Schleger, P. *Appl. Phys. A* **2002**, *74*, S361.
(12) Klein, J. *Macromolecules* **1986**, *19*, 105.
(13) Patri, A. K.; Majoros, I. J.; Baker, J. R., Jr. *Curr. Opin. Chem. Biol.* **2002**, *6*, 466.
(14) Li, Y.; Tseng, Y. D.; Kwon, S. Y.; d'Espaux, L.; Bunch, J. S.; McEuen, P. L.; Luo, D. *Nat. Mater.* **2004**, *3*, 38.
(15) Perkins, T. T.; Smith, D. E.; Chu, S. *Science* **1994**, *264*, 819.
(16) Smith, D. E.; Perkins, T. T.; Chu, S. *Phys. Rev. Lett.* **1995**, *75*, 4146.
(17) Smith, D. E.; Perkins, T. T.; Chu, S. *Macromolecules* **1996**, *29*, 1372.
(18) Käs, J.; Strey, H.; Sackmann, E. *Nature* **1994**, *368*, 226.
(19) Mills, P. J.; Mayer, J. W.; Kramer, E. J.; Hadziioannou, G.; Lutz, P.; Strazielle, C.; Rempp, P.; Kovacs, A. J. *Macromolecules* **1987**, *20*, 513.
(20) Roovers, J. *Macromolecules* **1988**, *21*, 1517.
(21) Griggiths, P. C.; Stilbs, P.; Yu, G. E.; Booth, C. *J. Phys. Chem.* **1995**, *99*, 16752.
(22) Schmidt, Th.; Schutz, G. J.; Baumgartner, W.; Gruber, H. J.; Schindler, H. *J. Phys. Chem.* **1995**, *99*, 17662.
(23) Anderon, C. M.; Georgiou, G. N.; Morrison, I. E. G.; Stevenson, G. V. W.; Cherry, R. J. *J. Cell Sci.* **1992**, *101*, 415.
(24) Fein, M.; Unkeless, J.; Chuang, F. Y. S., Sassaroli, M.; Costa, da R.; Vaananen, H.; Eisinger, J. *J. Membr. Biol.* **1993**, *135*, 83.
(25) Ghosh, R. N.; Webb, W. W. *Biophys. J.* **1994**, *66*, 1301.
(26) Ke, P. C.; Naumann, C. A. *Langmuir* **2001**, *17*, 3727.
(27) Efron, B.; Tibshirani, R. *Science* **1991**, *253*, 390.
(28) Musti, R.; Sikorav, J. L.; Lairez, D.; Jannink, G.; Adam, M. *C. R. Acad. Sci.* **1995**, Series II, *320*, 599, Part 1.
(29) Communications with: McLeish, T. C. B.; Larson, R. G.